Improvement of reproducible resistance switching in polycrystalline tungsten oxide films by in situ oxygen annealing

D. S. Shang, L. Shi, J. R. Sun, B. G. Shen, F. Zhuge, R. W. Li, and Y. G. Zhao

Improvement of reproducible resistance switching in polycrystalline tungsten oxide films by *in situ* oxygen annealing

D. S. Shang,[1,a)] L. Shi,[1] J. R. Sun,[1,b)] B. G. Shen,[1] F. Zhuge,[2] R. W. Li,[2] and Y. G. Zhao[3]

[1]*Beijing National Laboratory for Condensed Matter Physics and Institute of Physics, Chinese Academy of Sciences, Beijing 100190, People's Republic of China*
[2]*Ningbo Institute of Materials Technology and Engineering, Chinese Academy of Sciences, Ningbo, Zhejiang 315201, People's Republic of China*
[3]*Department of Physics and State Key Laboratory of New Ceramics and Fine Processing, Tsinghua University, Beijing 100084, People's Republic of China*

The electric-field-induced resistance switching in polycrystalline tungsten oxide films was investigated. Compared with the as-deposited film, the film annealed in an oxygen atmosphere shows a more stable switching behavior, a higher low-to-high resistance ratio, and a better endurance and retention. Based on the x-ray photoemission spectroscopy analysis, the resistance switching was attributed to the change in the interfacial barrier potential, due to the electron trapping/detrapping in the surface states, and the switching improvement was attributed to the decrease in the surface density of states. The present work suggests a possible approach controlling the resistance switching property by surface modification. © *2010 American Institute of Physics*. [doi:10.1063/1.3300637]

The phenomena associated with electric-field-induced resistance switching in the electrode/oxide/electrode structure have attracted great attention in the last decade due to their rich physics and potential application to the technique of resistive random access memory (RRAM), a technique for the next generation nonvolatile memory.[1] One of the most important challenges we faced is the physical origin for the resistance switching. Although many models have been proposed, the underlying physics is still not well understood.[2–4] A further important issue is the exploration of appropriate RRAM materials. Up to now, a large variety of materials have been found to show the characteristics of resistance switching, including binary and ternary transition-metal oxides, solid electrolytes, and organic materials.[5–11] Among them, the binary transition-metal oxides, such as NiO, TiO_2, and CuO_x, show very promising potential for the mass production of the RRAM devices because of their relatively simple composition, stoichiometric flexibility, and compatibility with the complementary-metal-oxide-semiconductor (CMOS) technology.[12] Furthermore, the transition-metal oxide can exhibit resistance switching in the polycrystalline structure. It therefore can be deposited on various substrates with different lattice constants and orientation, such as glass and plastic substrates. This will allow the designing of lightweight, flexible, and optic RRAM devices.

Tungsten oxide is an important wide band gap (2.57–3.25 eV, depending on the sample preparation) semiconductor with interesting physical and chemical properties, and has been widely studied for application, such as electrochromic devices, gas sensing, and catalysis.[13–16] Since tungsten is used as interconnect material between different metallization levels, tungsten oxide is compatible with the back-end-line process in the CMOS technology.[17] Recently, the resistance switching property has been reported in both Cu-doped amorphous tungsten oxide films by Kozicki *et al.*[17] and non-

stoichiometric tungsten oxide films prepared by plasma oxidation by Ho *et al.*[18] However, the mechanism for the resistance switching is still in dispute. Kozicki *et al.* attributed the resistance switching to localized Cu metal in the oxide, while Ho *et al.* ascribed this phenomenon to the localized state associated with oxygen vacancies. In this letter, we prepared polycrystalline tungsten oxide films on conductive glass substrates, and observed an improved reproducible resistance switching after oxygen annealing, this, together with the nonlinear current-voltage characteristics, suggests the dominant role of the barrier potential at the film-electrode interface.

Commercial glass sputtered with a $\sim$150 nm thick fluorine-doped tin oxide (FTO) thin film is used as a substrate and simultaneously bottom electrode. A tungsten oxide ceramic with the nominal composition of WO_3 was used as the target. Tungsten oxide films of $\sim$400 nm were deposited on the substrates by the pulsed laser deposition technique using a KrF excimer laser (λ=248 nm) with a repetition rate of 5 Hz and a fluence of 7 J/cm^2. During the deposition, the substrate temperature was maintained at 400 °C and the oxygen pressure was kept at 10 Pa. The sample we obtained is denoted as WO-1. A further *in situ* annealing at 400 °C for 30 min under an oxygen pressure of 0.1 MPa was performed for the WO-1 sample and the resultant sample is denoted as WO-2. The x-ray diffraction (XRD) pattern indicates that the films are polycrystalline. Atomic force microscopy (AFM) analysis shows uniform grains with the size of 120–150 nm in the films.[19] An Au electrode of $\sim$100 nm in thickness was deposited on the top of the WO_3 layer by ion sputtering. The size of the top electrode is 50×50 μm^2, defined by the photolithography and lift-off technique. Current-voltage (*I-V*) characteristics and resistance switching of the fabricated devices were measured by a Keithley SourceMeter 2601. The bias voltage was applied to the top electrode with the bottom electrode being grounded.

Figures 1(a) and 1(b) shows the *I-V* characteristics of the Au/WO-1/FTO device, measured by sweeping voltage in the

a)Electronic mail: shang_da_shan@163.com.
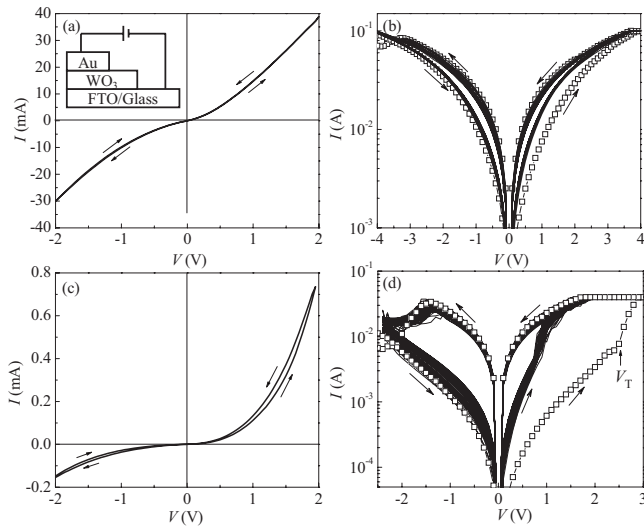b)Electronic mail: jrsun@g203.iphy.ac.cn.

FIG. 1. (a) and (c) show the *I-V* curves for the Au/WO-1/FTO and Au/WO-2/FTO devices, respectively, with a voltage sweep cycle of $0 \rightarrow 2$ V $\rightarrow -2$ V $\rightarrow 0$. Inset in (a) shows the schematic of the samples and the measurement. (b) and (d) show *I-V* curves with 100 cycles of voltage sweeping for the Au/WO-1/FTO and Au/WO-2/FTO devices, respectively. Open rectangle symbol denotes the first cycle of *I-V* curve.
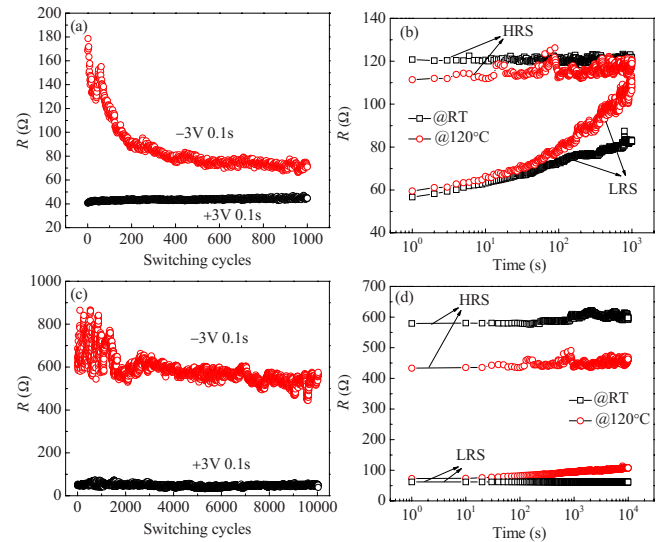

FIG. 2. (Color online) (a) and (c) show the electric-pulse-induced resistance switching of the Au/WO-1/FTO and Au/WO-2/FTO devices, respectively. (b) and (d) show the retention property of the resistance state of the Au/WO-1/FTO and Au/WO-2/FTO devices, respectively. The resistance values were measured at 0.2 V.

sequence of $0 \rightarrow V_{max} \rightarrow 0 \rightarrow -V_{max} \rightarrow 0$. The *I-V* curves show a weak rectifying characteristic when $V_{max}=2$ V, without hysteresis. By extending the sweeping range to $V_{max}=4$ V, a weak *I-V* hysteresis, which is repeatable up to 100 cycles, appeared, though the first cycle shows a somewhat different behavior. The *I-V* hysteresis indicates the resistance switching of the Au/WO-1/FTO devices between a low resistance state (LRS) and a high resistance state (HRS). In contrast, the Au/WO-2/FTO device shows a significant rectifying behavior in the sweeping region between -2 and 2 V [see Fig. 1(c)]. This means that the electronic transport was controlled by one of the electrode/film interfaces. With raising V_{max}, the current of the device exhibits a sudden increase at $V_T=-2.6$ V, which leads to a strong *I-V* hysteresis. The resistance change at V_T is called forming process, after which the device never went back to the initial resistance state (IRS).

The resistance switching triggered by electric pulses was further studied. Electric pulses of $+3$ and -3 V (pulse width$=0.1$ s) were alternatively applied to the devices and the resistance were measured at 0.2 V between two neighboring pulses. For the Au/WO-1/FTO devices, as shown in Fig. 2(a), the resistance of the HRS first reduced gradually with the number of switching cycles then stabilized in the state with a HRS/LRS ratio of $\sim$1.5. The retention measurement shows that the LRS is unstable and its resistance grows continuously with time. This feature is especially obvious at high temperatures, as shown in Fig. 2(b). For the Au/WO-2/FTO devices, the HRS to LRS resistance ratio is larger than ten, without considerable degradation after 10^4 cycles, which indicates a good endurance of the devices. The HRS and LRS obtained after 10^4 cycles were quite stable for more than 10^4 s even at 120 °C. These results reveal the reliability of Au/WO-2/FTO as a nonvolatile memory device.

The stoichiometric WO$_3$ is an *n*-type semiconductor with a work function of 5.1–6.4 eV.[20] Based on the semiconductor theory, no potential barrier could be formed at either the Au/WO$_3$ or the WO$_3$/FTO interface due to the lower work function of Au (5.1 eV) and FTO [4.4 eV (Ref. 21)], if

the surface states are neglectable.[22] However, the rectifying transport behaviors indicate the presence of a Schottky-type contact in the Au/WO-1 and the Au/WO-2 interface, identified from the rectifying direction. We also measured the *I-V* characteristics of the films with Ag (4.3 eV), indium tin oxide [4.4–4.8 eV, (Refs. 20 and 21)], and Pt (5.3 eV) electrodes, and similar rectifying behaviors were observed. These results indicate that the interface barrier may be exclusively determined by the surface states of the film, independent of electrode, and, furthermore, the resistance switching characteristics are closely related to surface states of the tungsten oxide films.

To get the information on surface state, an x-ray photoemission spectroscopy analysis (AXIS Ultra DLD, Shimadzu Corporation) with a monochromatic Al $K\alpha$ line was further performed. Figures 3(a) and 3(b) show the valance band and W 4*f* core level spectra of the WO-1 and WO-2 films, respectively. The valence band spectrum of the WO-1 (up curve) shows two main peaks. The first one between 2.5 and 10 eV arises from the O 2*p* and W 5*d* states, and the second one, which is close to the Fermi level, is associated with the W 5*d* states.[23] As well know, there is no electronic state near
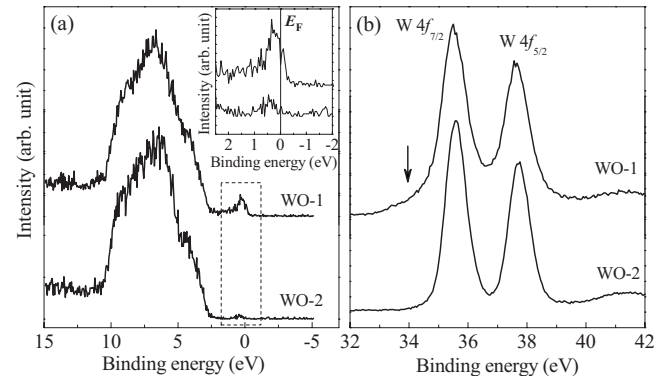

FIG. 3. (a) and (b) show the valence band and W 4*f* core level spectra of the samples, respectively. Inset shows the magnification of the boxed portion in (a).
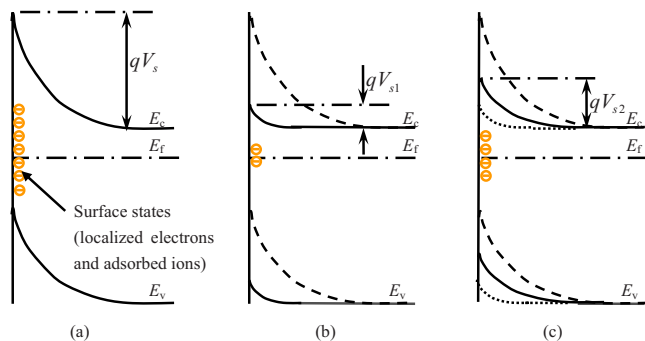
FIG. 4. (Color online) Schematic band diagrams of the WO$_3$ film surface based on the proposed mechanism of resistance switching in this study. (a), (b), and (c) represents the IRS, LRS, and HRS, respectively. E_c is the conduction band, E_v the valence band, and E_f the Fermi level, qV_s the surface potential barrier, and $qV_s > qV_{s2} > qV_{s1}$.

the Fermi level in stoichiometric WO$_3$.[23] The electronic states near the Fermi level in WO-1 could be an signature of the deviation of the oxygen content from stoichiometric value. Oxygen-annealing improved the oxygen stoichiometry of the sample, thus caused a density reduction of this state, as demonstrated by the data of WO-2. This is in agreement with the change in the W $4f$ core level spectra. As shown in Fig. 3(b), the W $4f$ core level spectrum is consist of the W $4f_{7/2}$ and W $4f_{5/2}$ doublet peaks, with the spin-orbit splitting energy of 2.1 eV.[24] However, an evident shoulder at the low energy side of the W $4f_{7/2}$ peak can be seen in the WO-1 sample [arrowed in Fig. 3(b)], due to the presence of W^{5+} (Ref. 25). This feature is not obvious in WO-2, which suggests a reduction in the density of the W^{5+} states after oxygen annealing.

Based on these results, a model for the resistance switching in WO$_3$ can be proposed. The existence of W $5d$ states near the Fermi level can be regarded as electron trap and ion adsorption centers at the film surface.[26] As a result, a negatively charged surface is formed, which causes a Schottky-type barrier (SB) by bending the energy bands near the film surface [Fig. 4(a)]. The trapped electrons at the surface states can be delocalized under high positive biases, which results in the decrease in the SB potential, thus the IRS-to-LRS switching [Fig. 4(b)]. On the contrary, the SB potential recovers partly under reverse biases due to the retrapping of the electrons. Consequently, the devices back to the HRS again [Fig. 4(c)]. Note that the device resistance cannot restore to the IRS in the switching process, probably due to some permanent changes in the SB during the forming process. The instable resistance switching behavior of the Au/WO-1/FTO devices can be ascribed to the surface metallic property due to the excessive surface density of states near the Fermi level, which causes large leakage current, and thus the instability of the formed SB during switching.[27] These explanations are similar to that proposed by Sawa *et al.*[28] However, the SB here is due to electron trapping and ion adsorbing, instead of a simple electrode/semiconductor contacting as occurred in the sample of Sawa *et al.* The present work indicates that the resistance switching can be significantly improved by a proper decoration of the film surface, though further studies are required for a thorough understanding of the resistance switching in tungsten oxide.

In summary, the resistance switching of two types of polycrystalline tungsten oxide films was investigated. The Au/WO-2/FTO devices show a more reliable resistance

switching behaviors with a larger HRS/LRS ratio, better endurance, and retention than that of the Au/WO-1/FTO devices. The resistance switching was discussed based on the change in interfacial barrier potential induced by the electron trapping/detrapping in the surface states and the switching improvement was attributed to the decrease in surface density of states. The present results suggest a possible way to improve the resistance switching performance by the film surface modification.

[1] R. Waser and M. Aono, Nat. Mater. **6**, 833 (2007).
[2] K. Szot, W. Speier, G. Bihlmayer, and R. Waser, Nat. Mater. **5**, 312 (2006).
[3] A. Sawa, Mater. Today **11**, 28 (2008).
[4] J. J. Yang, M. D. Pickett, X. M. Li, D. A. A. Ohlberg, D. R. Stewart, and R. S. Williams, Nat. Nanotechnol. **3**, 429 (2008).
[5] B. J. Choi, D. S. Jeong, S. K. Kim, S. Choi, J. H. Oh, C. Rohde, H. J. Kim, C. S. Hwang, K. Szot, R. Waser, B. Reichenberg, and S. Tiedke, J. Appl. Phys. **98**, 033715 (2005).
[6] S. Seo, M. J. Lee, D. H. Seo, E. J. Jeoung, D. S. Suh, Y. S. Young, I. K. Yoo, I. S. Byun, I. R. Hwang, S. H. Kim, I. S. Byun, J. S. Kim, J. S. Choi, and B. H. Park, Appl. Phys. Lett. **85**, 5655 (2004).
[7] A. Chen, S. Haddad, Y. C. Wu, T. N. Fang, S. Kaza, and Z. Lan, Appl. Phys. Lett. **92**, 013503 (2008).
[8] A. Beck, J. G. Bednorz, Ch. Gerber, C. Rossel, and D. Widmer, Appl. Phys. Lett. **77**, 139 (2000).
[9] S. Q. Liu, N. J. Wu, and A. Ignatiev, Appl. Phys. Lett. **76**, 2749 (2000).
[10] M. N. Kozicki, M. Park, and M. Mitkova, IEEE Trans. Nanotechnol. **4**, 331 (2005).
[11] J. C. Scott and L. D. Bozano, Adv. Mater. **19**, 1452 (2007).
[12] M. J. Lee, Y. Park, D. S. Suh, E. H. Lee, S. Seo, D. C. Kim, R. Jung, B. S. Kang, S. E. Ahn, C. B. Lee, D. H. Seo, Y. K. Cha, I. K. Yoo, J. S. Kim, and B. H. Park, Adv. Mater. **19**, 3919 (2007).
[13] K. Miyake, H. Kaneko, M. Sano, and N. Suedomi, J. Appl. Phys. **55**, 2747 (1984).
[14] C. G. Granqvist, Sol. Energy Mater. Sol. Cells **60**, 201 (2000).
[15] T. Siciliano, A. Tepore, G. Micocci, A. Serra, D. Manno, and E. Filippo, Sens. Actuators B **133**, 321 (2008).
[16] I. E. Wachs, T. Kim, and E. I. Ross, Catal. Today **116**, 162 (2006).
[17] M. N. Kozicki, C. Gopalan, M. Balakrishnan, and M. Mitkova, IEEE Trans. Nanotechnol. **5**, 535 (2006).
[18] C. H. Ho, E. K. Lai, M. D. Lee, C. L. Pan, Y. D. Yao, K. Y. Hsieh, R. Liu, and C. Y. Lu, IEEE Symposium on VLSI Technology Digest, IEEE, Kyoto, 2007 (unpublished), p. 228.
[19] See supplementary material at http://dx.doi.org/10.1063/1.3300637 for the results of the XRD and AFM analyses.
[20] J. Meyer, S. Hamwi, T. Bülow, H. H. Johannes, T. Riedl, and W. Kowalsky, Appl. Phys. Lett. **91**, 113506 (2007).
[21] A. Andersson, N. Johansson, P. Bröms, N. Yu, D. Lupo, and W. R. Salaneck, Adv. Mater. **10**, 859 (1998).
[22] S. M. Sze and K. K. Ng, *Physics of Semiconductor Devices*, 3rd ed. (Wiley, New Jersey, 2007).
[23] F. J. Himpsel, J. F. Morar, F. R. McFeely, and R. A. Pollak, Phys. Rev. B **30**, 7236 (1984).
[24] T. H. Fleisch and G. J. Mains, J. Chem. Phys. **76**, 780 (1982).
[25] S. Santucci, L. Lozzi, E. Maccallini, M. Passacantando, L. Ottaviano, and C. Cantalini, J. Vac. Sci. Technol. A **19**, 1467 (2001).
[26] J. Guérin, K. Aguir, and M. Bendahan, Sens. Actuators B **119**, 327 (2006); A. Varpula, S. Novikov, J. Sinkkonen, and M. Utriainen, *ibid.* **131**, 134 (2008).
[27] T. K. Gupta and W. G. Carlson, J. Appl. Phys. **53**, 7401 (1982); S. Hirose, A. Nakayama, H. Niimi, K. Kageyama, and H. Takagi, *ibid.* **104**, 053712 (2008).
[28] A. Sawa, T. Fujii, M. Kawasaki, and Y. Tokura, Appl. Phys. Lett. **85**, 4073 (2004).